Journal of Chromatography A, 1216 (2009) 5548–5556

Contents lists available at ScienceDirect

Journal of Chromatography A

journal homepage: www.elsevier.com/locate/chroma

Engineering properties of a camelid antibody affinity sorbent for Immunoglobulin G purification

Marlene Zandian, Alois Jungbauer*

Department of Biotechnology, University of Applied Life Sciences and Natural Resources Vienna, Muthgasse 18, A-1190 Vienna, Austria

ARTICLE INFO

Article history:
Received 11 March 2009
Received in revised form 18 May 2009
Accepted 20 May 2009
Available online 29 May 2009

Keywords:
Pore diffusion
Dynamic binding capacity
Surface plasmon resonance kinetics
Antibody fragment

ABSTRACT

An IgG-specific camelid antibody matrix (BAC, Naarden, The Netherlands), developed from an immune phage display library, was characterized regarding engineering properties including mass transfer characteristics. Uptake kinetics and equilibrium binding capacity were determined by a finite bath method. Adsorption kinetic parameters were also determined using a real time biosensor. Slightly different properties to conventional Staphylococcal protein A affinity media were shown; especially a 2–2.5 times lower maximal binding capacity with a value of 26 mg/ml polyclonal IgG was obtained. Mass transfer could be described by using a film and pore diffusion model ($D_e = 5 \times 10^{-8}$ cm^2/s). Determined engineering parameters were used to predict breakthrough behaviour in column mode considering film and pore resistances. The dynamic binding capacity at 10% breakthrough did not change when residence time was at least 6 min.

1. Introduction

The discovery of unique type of antibodies, which are found in camels, dromedaries and llamas (*Camelidae*), has enabled the development of alternative ligands for affinity chromatography processes [1]. To date, no detailed information on the engineering parameters including mass transfer characteristics of camelid affinity matrices have been reported. The most important parameters for engineering an affinity chromatography process are the maximum binding capacity, adsorption parameters and the effective diffusivity. These data are obtained by approximation of adsorption isotherm and uptake kinetic measurements. From these parameters and parameters characterizing the morphology of the stationary phase (particle diameter, intraparticle porosity) breakthrough behaviour can be predicted and compared to experimental data. The plot of dynamic binding capacity at 10% breakthrough versus residence time has been applied as a very useful tool to design an affinity chromatography column [2].

In the last two decades Staphylococcal protein A (SpA) affinity chromatography has been established as the standard unit operation for purification of therapeutic antibodies. SpA suffers from several drawbacks. The primary misgivings are the high handling cost, safety and stability aspects [3,4]. Furthermore, it lacks specificity for IgG_3 subclass, which would also be important for extracorporeal immunoadsorption in treatment of some autoimmune diseases [5–7]. Therefore, and due to the very attractive market opportunity, extensive efforts into finding alternative cost-effective and reliable chromatographic or non-chromatographic processes for antibody purification were investigated.

The bioaffinity company BAC (Naarden, The Netherlands) in collaboration with GE Healthcare (Uppsala, Sweden) has developed an IgG affinity matrix using a camelid heavy chain antibody as ligand generated from an immune phage display library. Camelid antibodies (also termed VHH antibodies) are formed by two heavy chains with one single variable domain and lack the light chain. With a size of 13 kDa, they represent the smallest antigen binding domain and are able to recognize new targets, which are not accessible for conventional antibodies [8]. In addition to the benefits of easy cloning, high stability and solubility, this ligand has the advantage over SpA, that it binds all IgG subclasses including IgG_3. Furthermore, no cross reactivity neither with other human plasma proteins, nor with IgG from other species could be determined [9]. When immobilizing these antibodies onto conventionally used porous matrices with a pore diameter of approximately 50–100 nm, a limited pore diffusion result can be expected. Several groups could describe the adsorption of IgG on SpA by a pore diffusion limited process [2,10].

To date, no information on the engineering parameters of CaptureSelect human-Fc affinity matrix have been reported. In the present work, the CaptureSelect human-Fc matrix was evaluated in comparison to SpA affinity matrices. The uptake kinetics and equilibrium binding capacity was determined by a finite bath method. Adsorption kinetic parameters from uptake experiments were also compared to them using a real time biosensor.

* Corresponding author. Tel.: +43 1 36006 6226; fax: +43 1 3697615.
E-mail address: alois.jungbauer@boku.ac.at (A. Jungbauer).

0021-9673/$ – see front matter © 2009 Elsevier B.V. All rights reserved.
doi:10.1016/j.chroma.2009.05.051

2. Materials and methods

2.1. Materials

CaptureSelect human-Fc affinity matrix and CaptureSelect human IgG ligand were purchased from BAC. All experiments were performed with human polyclonal IgG, which was kindly provided by Octapharma (Vienna, Austria). Chemicals and solvents used for buffer preparation and analysis were of analytical grade and if not otherwise specified purchased from Merck (Darmstadt, Germany). All experiments were carried out using phosphate buffered saline (PBS) containing 140 mM NaCl, 2.7 mM KCl, 81 mM Na_2HPO_4, 18 mM KH_2PO_4 at room temperature.

2.2. Batch adsorption isotherm

0.1 ml of a 50:50 (v/v) gel suspension was equilibrated in PBS. IgG solutions with various concentrations between $C_0 = 0.05$ and 3 mg/ml were prepared and added to the gel samples until an absolute IgG content of 2 mg/ml was reached. The suspensions were gently rotated by a head-over-head rotator (Stuart rotator SB3, Bibby Sterilin, Stone, UK) in appropriate reaction vessels in order to avoid IgG precipitation. After 6 and 24 h equilibration, respectively, IgG content of the mobile phase was analyzed by measuring the UV absorbance on a spectrophotometer (Cary 50 Bio, Varian Instruments, Darmstadt, Germany) at 280 nm. The calculated concentration of IgG per ml of stationary phase was plotted against the concentration of IgG in the mobile phase. Data were approximated with the Langmuir isotherm model to obtain the maximal binding capacity q_{max} and the dissociation constant K_D.

2.3. Batch uptake kinetics

Uptake kinetics were performed under finite bath conditions at $C_0 = 1$ mg/ml and $C_0 = 0.1$ mg/ml IgG. PBS was used for gel equilibration and sample preparation. The amount of resin and IgG solutions were chosen in a manner that ensured a greater than 40% excess of IgG in the mobile phase after reaching equilibrium. The suspensions were gently rotated in appropriate reaction vessels in order to avoid IgG precipitation. Samples were drawn from the suspension after various time intervals within a time period of 24 h and were immediately filtrated (0.2 μm Millex GV, Millipore, Bedford, MA, USA) to remove resin particles. Samples were analyzed photometrically at 280 nm to determine the IgG concentration in the mobile phase. The concentration of IgG per ml of stationary phase was plotted against the time of sampling. Data were fitted with the lumped kinetic model to obtain the adsorption rate constant k_a. Effective diffusivity D_e was estimated using the pore and film diffusion model for batch adsorption introduced by Teo and Ruthven [11].

2.4. Breakthrough experiments

Chromatographic experiments were conducted using an ÄKTAexplorer 100 system (GE Healthcare, Uppsala, Sweden). CaptureSelect human-Fc affinity matrix was flow packed at a velocity of 800 cm/h in Tricorn 5 columns (GE Healthcare) to a bed height of 10 cm. Breakthrough experiments were performed with PBS at 0.4 and 1 mg/ml IgG and different flow velocities (50, 75, 100, 150, 200, 300, 400, 600 cm/h). IgG was eluted with 0.1 M Glycine–HCl pH 3.0 and the column was regenerated with 0.1 M Glycine–HCl pH 2.0. Dynamic binding capacity at 10% breakthrough (DBC10%) as a function of residence time was fitted with the model for pore diffusion from Cooper and Liberman [12] and Carta et al. [13] to obtain the effective diffusivity D_e and an apparent maximum binding capacity.

2.5. Biacore kinetic measurements

Kinetic measurements were carried out on a surface plasmon resonance system (Biacore 2000, Uppsala, Sweden) at 25 °C using PBS-T (PBS containing 0.005% Tween-20) as the running and sampling buffer. Polyclonal IgG was immobilized onto a CM5 chip sensor surface by *N*-(3-dimethylaminopropyl)-*N*′-ethylcarbodiimide (EDC) and *N*-hydroxysuccinimide (NHS) chemistry with an amount of approximately 1000 RU. Various concentrations of free CaptureSelect human IgG ligand were injected across the sensor surface. The obtained sensorgrams were substracted from the sensorgrams of a blank cell and evaluated with the Biaevaluation software (Biacore) by using the Langmuir 1:1 binding model.

3. Theory

3.1. Batch adsorption in finite bath—lumped kinetic model

The 1:1 interaction of an immobilized ligand (A) and its adsorbate (B) in solution can be simply described with an equilibrium relationship of the form:

$$A + B \underset{k_d}{\overset{k_a}{\rightleftharpoons}} AB \tag{1}$$

where k_a and k_d represents the "lumped" kinetic rate constants of association and dissociation, respectively, which include all mass transfer resistances (film diffusion, solid diffusion, pore diffusion and surface reaction resistance). The ratio of k_d/k_a represents the dissociation constant K_D.

The net rate of complex formation is given by the Langmuir kinetic model [14] with:

$$\frac{dq}{dt} = k_a c(q_{max} - q) - k_d q \tag{2}$$

where q is the adsorbed protein concentration, t the time, c the concentration of adsorbate in mobile phase and q_{max} the maximum binding capacity of the adsorbent.

At equilibrium, where $dq/dt = 0$, Eq. (2) can be written as:

$$q = \frac{q_{max} c}{K_D + c} \tag{3}$$

representing the most commonly used non-linear isotherm based on the work of Irving Langmuir, regarding gas–solid interactions on the basis of the Gibbs isotherm [15]. The dimensionless separation factor R for the Langmuir isotherm is described as:

$$R = \frac{1}{1 + KC_{ref}} \tag{4}$$

where C_{ref} represents a reference concentration. The isotherm is linear when $R = 1$ and rectangular or irreversible when $R = 0$ [16]. The Langmuir isotherm model assumes an ideal adsorption layer, monolayer coverage and the lack of interactions between the adsorbates.

For batch adsorption in a stirred tank, Skidmore et al. [17] introduced an analytical solution (Eqs. (5)–(7)) based on the work of Chase [18] (Eq. (2)) describing the adsorption of proteins to affinity adsorbents by one single lumped adsorption rate constant k_a, namely the kinetic rate constant model:

$$c = C_0 - \frac{v}{V}\left[\frac{(b+a)(1 - \exp\{-(2av/V)k_a t\})}{((b+a)/(b-a)) - \exp\{-(2av/V)k_a t\}}\right] \tag{5}$$

$$a^2 = b^2 - \left(\frac{C_0 V}{v}\right) q_{max} \tag{6}$$

$$b = \frac{1}{2}\left(\frac{C_0 V}{v} + q_{max} + \frac{K_D V}{v}\right) \tag{7}$$

with C_0 as the initial mobile phase protein concentration, v as the volume of the adsorbate and V as the volume of the mobile phase.

3.2. Batch adsorption in finite bath—film and pore diffusion model

For batch adsorption in finite bath Teo and Ruthven [11] introduced an analytical solution for film and pore diffusion. The model can be used for rectangular isotherms when R is small:

$$\left(\frac{C_0}{q_s}\right)\left(\frac{D_e t}{r_p^2}\right) = \left(1-\frac{1}{B_i}\right) I_2 - I_1 \tag{8}$$

where:

$$I_1 = \frac{1}{6\lambda\Lambda}\ \ln\left[\left(\frac{\lambda^3+\eta^3}{\lambda^3+1}\right)\left(\frac{\lambda+1}{\lambda+\eta}\right)^3\right] + \frac{1}{\lambda\Lambda\sqrt{3}}\left[\tan^{-1}\left(\frac{2\eta-\lambda}{\lambda\sqrt{3}}\right) - \tan^{-1}\left(\frac{2-\lambda}{\lambda\sqrt{3}}\right)\right] \tag{9}$$

$$I_2 = \frac{1}{3\Lambda}\ \ln\left(\frac{\lambda^3+\eta^3}{\lambda^3+1}\right) \tag{10}$$

$$\Lambda = \frac{v q_{max}}{V C_0} \tag{11}$$

$$\eta = \left(1-\frac{\bar{q}}{q_{max}}\right)^{1/3} \tag{12}$$

$$\lambda = \left(\frac{1}{\Lambda}-1\right)^{1/3} \tag{13}$$

$$B_i = \frac{k_f r_p}{D_e} \tag{14}$$

with C_0 as the initial mobile phase protein concentration, q_s as the adsorbed-phase concentration, D_e as the effective diffusivity, t as the time, r_p as the particle radius, Λ as the fraction of adsorbed protein at equilibrium, v as the volume of the adsorbate, V as the volume of the mobile phase, $\bar{q}$ as the average concentration in particle, q_{max} as the maximum monolayer capacity and k_f as the film mass transfer coefficient. B_i represents the dimensionless Biot number, which is used to describe the relative importance of intraparticle and external film resistance. An usual $B_i > 10$ indicates that the external resistance is negligible. D_e represents the effective pore diffusivity which is typically smaller than the free solution protein diffusivity D_0, caused by the porosity, by the tortuosity of the pore and by steric hindrances, which depend on the ratio of solute size to pore size.

The film mass transfer coefficient k_f can be estimated from Sherwood number correlations described, *e.g.* by Wilson and co-workers [16,19] where:

$$Sh = \frac{k_f d_p}{D_0} = \frac{1.09}{\varepsilon}\left(\frac{u d_p}{D_0}\right)^{0.33} \tag{15}$$

3.3. Frontal analysis—constant pattern solution for film and pore diffusion

Measurements in column mode gave the most relevant parameters for design and scale up of an industrial process. Breakthrough curves can be predicted by the pore diffusion solution given by Weber and Chakravorti [20]. The model can be used for rectangular isotherms which ensure constant pattern behaviour and considers pore diffusion and film resistances in series:

$$N_{pore}(\tau_1 - 1) = \frac{15}{\sqrt{3}}\ \tan^{-1}\left[\frac{2(1-X)^{1/3}+1}{\sqrt{3}}\right] - \frac{15}{2}\ \ln\left[1+(1-X)^{1/3}+(1-X)^{2/3}\right] + \left(\frac{N_{pore}}{N_{film}}\right)[\ln(X)+1] - \frac{5\pi}{2\sqrt{3}} + \frac{5}{2} \tag{16}$$

where:

$$X = \frac{C_{out}}{C_F} \tag{17}$$

$$\tau_1 = \left(\frac{ut}{L}-\varepsilon\right)\left(\frac{C_F}{(1-\varepsilon)q_{max}}\right) \tag{18}$$

$$N_{pore} = \left(\frac{60(1-\varepsilon)D_e}{d_p^2}\right)\left(\frac{L}{u}\right) \tag{19}$$

$$N_{film} = \left(\frac{6(1-\varepsilon)k_f}{d_p}\right)\left(\frac{L}{u}\right) \tag{20}$$

C represents the sample outlet concentration and C_f is the sample feed concentration. τ_1 represents the dimensionless time, with u as superficial velocity, t as time, L as column length, ε as external void fraction and q_{max} as maximum binding capacity. N_{pore} and N_{film} are representative values for pore diffusion and film diffusion. D_e is the effective diffusivity, d_p is the particle diameter and k_f represents the film mass transfer coefficient. Several analytical constant pattern solutions where published for $R < 1$ considering film diffusion, pore diffusion, solid diffusion, linear driving force, axial dispersion and reaction kinetics [16]. The constant pattern condition for a rectangular isotherm is achieved if $N\tau_1 > 2.5$. N describes the number of transfer units, $N = L/\mathrm{HTU}$, where HTU is the height of a transfer unit. When the solution concentration is small in comparison to the adsorption capacity, the dimensionless time τ_1 can be simplified as described by the following equation:

$$\frac{DBC}{(1-\varepsilon)q_F} = \tau_1 \tag{21}$$

where $(1-\varepsilon)q_F$ describes the equilibrium binding capacity (EBC). DBC represents the dynamic binding capacity. For $C/C_F = 0.1$ (dynamic binding capacity at 10% breakthrough; DBC10%) at constant pattern condition the pore diffusion model of Cooper and Liberman [12] (simplified form of Eq. (16); without film diffusion) yields:

$$\tau_1 = \frac{1-1.03}{N} \tag{22}$$

By plotting the ratio of DBC10% and EBC versus residence time, data can be approximated using Eqs. (19) and (22) and the effective diffusivity D_e can be calculated.

A general solution for non constant pattern condition (short residence time) published by Carta et al. [13] is given by:

$$\tau_1 \sim 0.364N - 0.0612N^2 + 0.00423N^3 \tag{23}$$

4. Results and discussion

4.1. Adsorption isotherm

Adsorption isotherm was measured using polyclonal IgG with a typical batch uptake method in PBS at room temperature. Previous experiences with SpA media have shown that they attain full saturation very slowly, particularly at low IgG concentrations. Several explanations were described for this phenomenon; changing of the transport mechanism due to pore radius reduction during adsorption [21], IgG aggregates which are competing with monomer IgG molecules [22], or stretching of the IgG molecule [23]. Therefore,

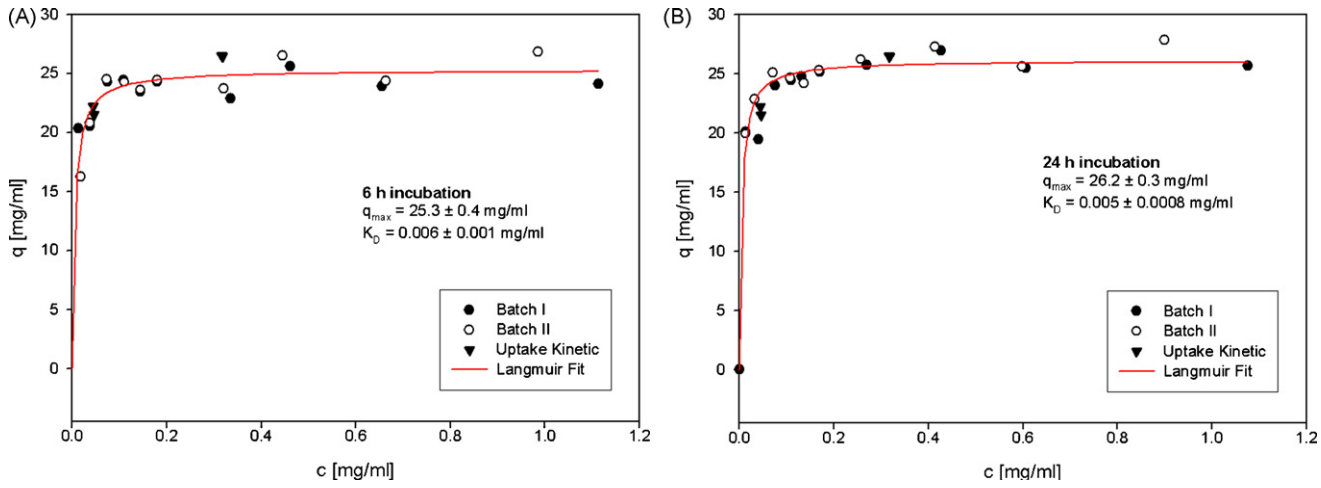

Fig. 1. Adsorption isotherm of polyclonal IgG adsorbed per ml CaptureSelect human-Fc affinity matrix. Data from batch adsorption and uptake kinetics were approximated with the Langmuir isotherm model. (A) Adsorption isotherm after 6 h equilibration. (B) Adsorption isotherm after 24 h equilibration.

adsorption isotherm was performed using two different incubation times, 6 and 24 h, respectively. Due to the tendency of polyclonal IgG to aggregate with time, reaction tubes and mixing velocity were chosen in a manner that limited shear stress (low rpm and a low ratio of air to solute in the tube). As shown in Fig. 1 the isotherm of the CaptureSelect human-Fc affinity matrix represents a very favourable and almost rectangular isotherm. Data fit well to the Langmuir isotherm model (Eq. (3)) resulting in similar characteristic parameter values for both measurements (summarized in Table 1). Equilibrium data from batch uptake kinetic measurements (described in the next section) were also included for the Langmuir approximation. The resulting K_D value of ~0.005 mg/ml or $\sim 3.3 \times 10^{-8}$ M (M.W. of IgG: 150,000 Da), respectively is nearly one order of magnitude lower than published K_D values from SpA affinity sorbents [2], such as MabSelect type (GE Healthcare) and ProSep-vA type (Millipore). This is attributed to an underestimation of K_D of SpA affinity media. Published isotherms were measured using an equilibration time of just 3 h. Therefore, particularly at low concentrations, equilibrium conditions were not reached. The actual isotherm would be steeper and the K_D value lower. Nevertheless, the maximum equilibrium binding capacity of approximately 26 mg/ml IgG is 2–2.5 times lower than for SpA matrices [2]. The explanation could be that camelid VHH antibodies are monomeric molecules, whereas SpA has a theoretical valency of five, in fact a valency of 2–3 was determined in practice. Thus, they are not able to bind multiple IgGs. This may result in a capacity limitation [24]. Two more factors can give rise to the low capacity: (1) ligand coupling density is a main factor influencing adsorption capacity. This adsorbent may have low ligand density. (2) The matrix has large pore size that leads to low specific surface area, which may also be the reason for low ligand coupling density.

Table 1
Summary: engineering parameters CaptureSelect human-Fc affinity matrix.

Isotherm			
q_{max} at 6 h (mg/ml)	K_D at 6 h (mg/ml)	q_{max} at 24 h (mg/ml)	K_D at 24 h (mg/ml)
25.3 ± 0.4	0.006 ± 0.001	26.2 ± 0.3	0.005 ± 0.0008
Batch uptake kinetic			
k_a (mL/mg s)	D_e at C_0 = 0.1 mg/ml IgG (cm^2/s)		D_e at C_0 = 1 mg/ml IgG (cm^2/s)
0.0036 ± 0.0004	5.0×10^{-8}		4.7×10^{-8}
Frontal analysis			
D_e at C_0 = 0.4 mg/ml IgG (cm^2/s)		D_e at C_0 = 1 mg/ml IgG (cm^2/s)	
5.1×10^{-8}		5.0×10^{-8}	

4.2. Batch uptake kinetics

Batch uptake kinetics were performed as finite bath experiments at C_0 = 1 mg/ml and C_0 = 0.1 mg/ml polyclonal IgG. The IgG uptake at different times in terms of IgG capacity per ml of settled gel particles and in terms of dimensionless solution concentration (C/C_0) is shown in Fig. 2. In order to determine the mass transfer mechanism, experimental data were approximated with both the kinetic rate constant model published by Skidmore et al. [17] (Fig. 2) and the film and pore diffusion model for batch adsorption published by Teo and Ruthven [11] (Fig. 3). The former was used for the estimation of the association rate constant k_a. The isotherm parameters q_{max} and K_D, which were determined in the batch isotherm experiments described above, were taken for the approximation. A k_a of 0.0036 ± 0.0004 mL/g s or 540 ± 60 M^{-1} s^{-1}, respectively, could be obtained for both concentrations (Table 1). The effective diffusivity D_e was estimated by fitting the batch uptake data to the film and pore diffusion model (Fig. 3). The approximation was not feasible over the entire time, because the model only describes a certain parameter range. Thus, q_{max} was matched according to the time, which resulted in best fits as shown in Fig. 3. An effective diffusivity D_e of approximately 5×10^{-8} cm^2/s could be obtained at both C_0 = 0.1 mg/ml and C_0 = 1 mg/ml polyclonal IgG (summarized in Table 1). The free solution diffusivity D_0 of IgG was estimated by the correlation from Tyn and Gusek [25] with 5×10^{-7} cm^2/s. D_e is typically smaller than D_0, due to the porosity of the matrix, the tortuosity of the pore and steric hindrances, which depend on the ratio of solute size to pore size. The calculated ratio D_e/D_0 gives a value of 0.1, which corresponds to the theory. Hahn et al. [2], Horstmann and Chase [26] and McCue et al. [10] determined D_e values which are inversely proportional to the feed concentration for SpA sorbents, in a range of, *e.g.* 5–35 $\times 10^{-8}$ cm^2/s in the case of MabSelectXtra. It was assumed that this behaviour is caused by not reaching equilibrium in isotherm and uptake kinetic experiments, as mentioned in the previous section. This phenomenon could not be observed for the CaptureSelect human-Fc affinity matrix, where isotherm and uptake kinetic measurements were performed within a time period of 24 h.

The adsorption time to reach equilibrium can be calculated with the following equation:

$$t_\theta = \frac{-\ln(1-\theta)}{k_a \times C + k_d} \quad (24)$$

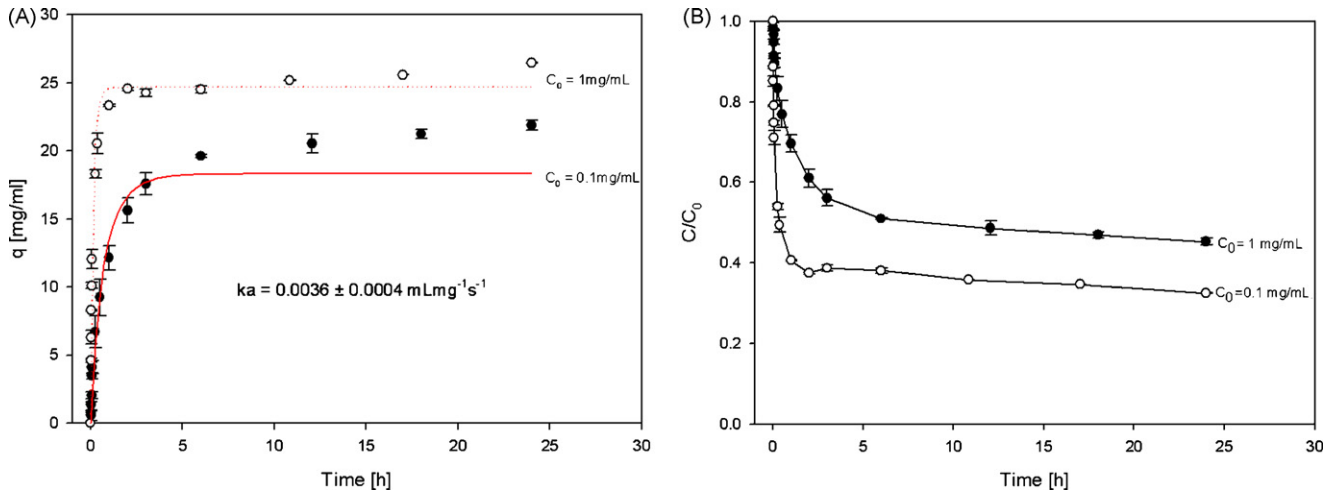

Fig. 2. Batch adsorption kinetics of polyclonal IgG on CaptureSelect human-Fc affinity matrix at C_0 = 0.1 mg/ml and C_0 = 1 mg/ml. (A) Amount of protein adsorbed (capacity q) versus time. Data were approximated with the kinetic rate constant model resulting in an association rate constant value of 0.0036 ± 0.0004 mL/g s. (B) Dimensionless solution concentration C/C_0 versus time.

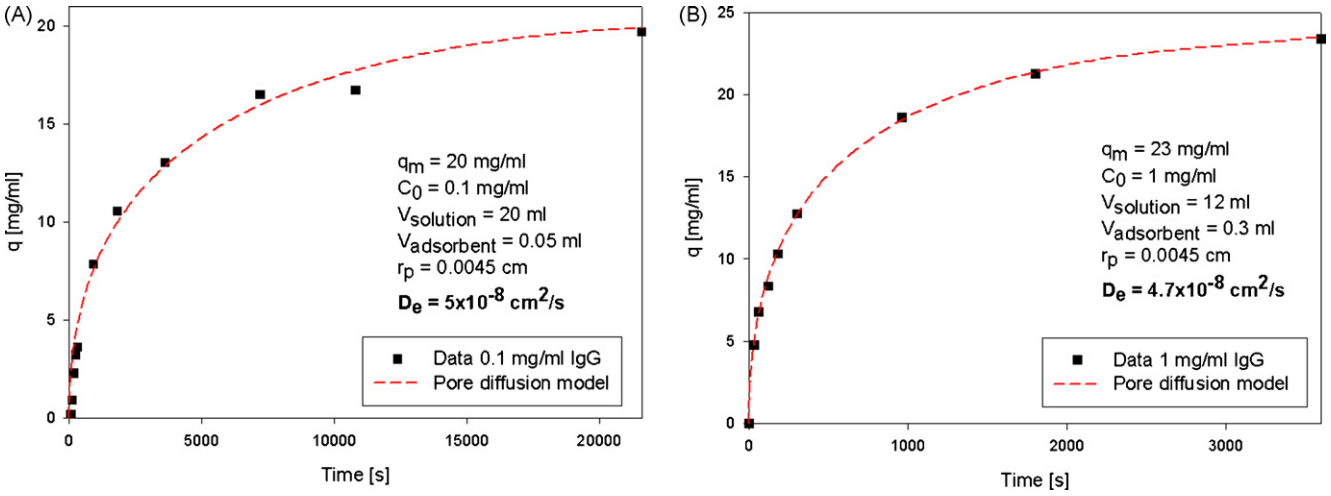

Fig. 3. Batch uptake kinetics at C_0 = 0.1 mg/ml (A) and at 1 mg/ml polyclonal IgG (B). Experimental data where approximated with the batch film and pore diffusion model described by Teo and Ruthven [11].

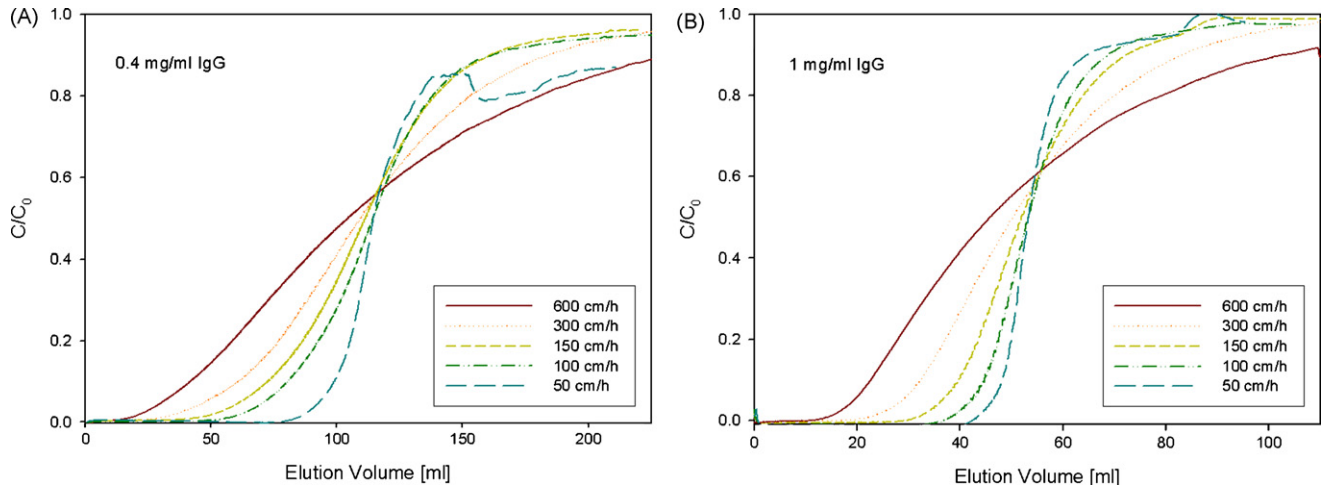

Fig. 4. Breakthrough curves of polyclonal IgG on CaptureSelect human-Fc affinity matrix at 0.4 mg/ml (A) and 1 mg/ml (B) and at different flow velocities.

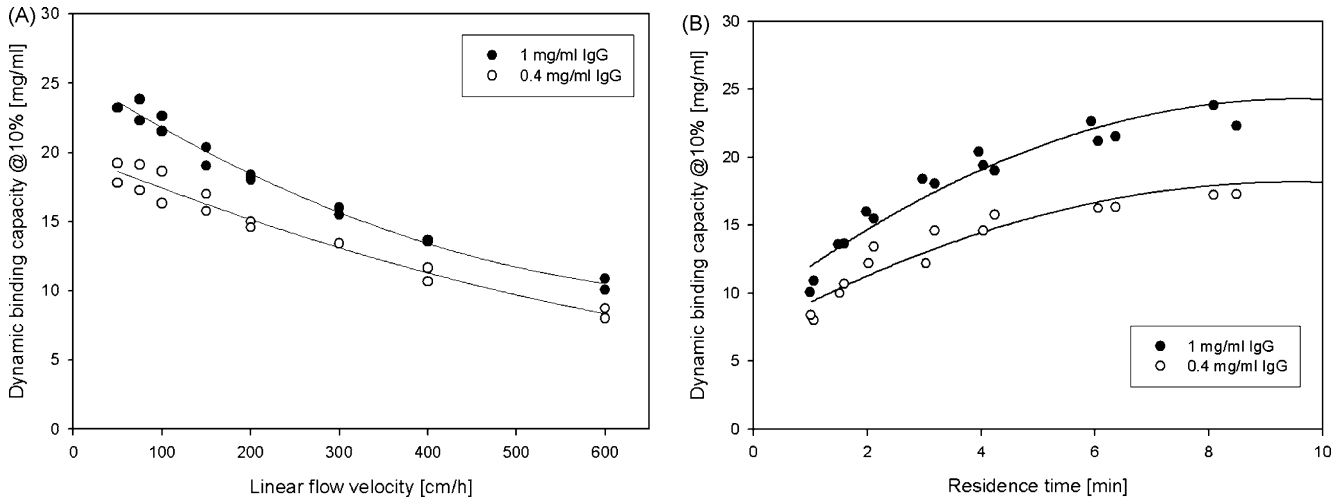

Fig. 5. Dynamic binding capacity at 10% breakthrough (DBC10%) in relation to linear flow velocity (A) and in relation to residence time (B) at 0.4 and 1 mg/ml polyclonal IgG.

where $\theta = q/q_{max}$. The ratio of k_d/k_a represents the dissociation constant K_D. With the values estimated in batch isotherm and uptake kinetics, a k_d value of $\sim 2.2 \times 10^{-5}\ s^{-1}$ can be calculated. Thus, at a concentration of 1 mg/ml IgG, 90% of equilibrium is reached in 10.6 min. At a concentration of 0.1 mg/ml, 90% of equilibrium is reached in 1.7 h. Consequently the incubation time used for isotherm measurements was sufficiently long.

4.3. Frontal analysis

Measurements in column mode provide the most relevant parameters for design and scale up of process chromatography. Breakthrough curves were performed at different velocities and polyclonal IgG concentrations in Tricorn 5 columns with a bed height of approximately 10 cm. Breakthrough profiles at 0.4 and 1 mg/ml IgG are depicted in Fig. 4. The dependence of dynamic binding capacity at 10% breakthrough (DBC10%) upon velocity and residence time of the sample is shown in Fig. 5, indicating mass transfer limitations. The DBC10% decreases nearly linear with increasing flow velocity. At residence times greater than 6 min the DBC10% approaches the equilibrium binding capacity. This is considered as the optimal operation point of the column. With a greater residence time only a marginal gain in capacity is achieved, but with severe loss of productivity.

The column void fraction determined with an inert large molecule (plasmid DNA; 4.9 kbp) was 0.38. In order to estimate effective diffusivity, dimensionless time τ_1 (DBC10% versus EBC) was plotted against residence time and approximated with the constant pattern solution and the general solution as described in Section 3 (Eqs. (19), (22) and (23); Fig. 6). The approximated EBC was lower than the maximum binding capacity obtained from the batch isotherm experiments. The explanation is that the model does not describe the saturation phase well. Particularly with regard to IgG, which reaches equilibrium relatively slowly, the calculation of EBC is affected. However, in both cases, at 0.4 and 1 mg/ml IgG, an effective diffusivity of approximately $5 \times 10^{-8}\ cm^2/s$ could be determined (Table 1). This corresponds to the data obtained from approximation of the pore and film diffusion model to the batch uptake data, as described above. Hahn et al. [2] calculated comparable D_e values for SpA media using the same model, indicating similar mass transfer behaviour. Table 1 summarizes engineering parameters obtained from batch and column experiments.

By using the determined D_e from the pore diffusion model breakthrough curves were predicted with the film and pore diffusion model under constant pattern conditions by Weber and Chakravorti [20] (Fig. 7). The breakthrough prediction fits well at 1 mg/ml IgG concentration, indicating a pore diffusion limited process. At 0.4 mg/ml IgG breakthrough prediction would be more precisely

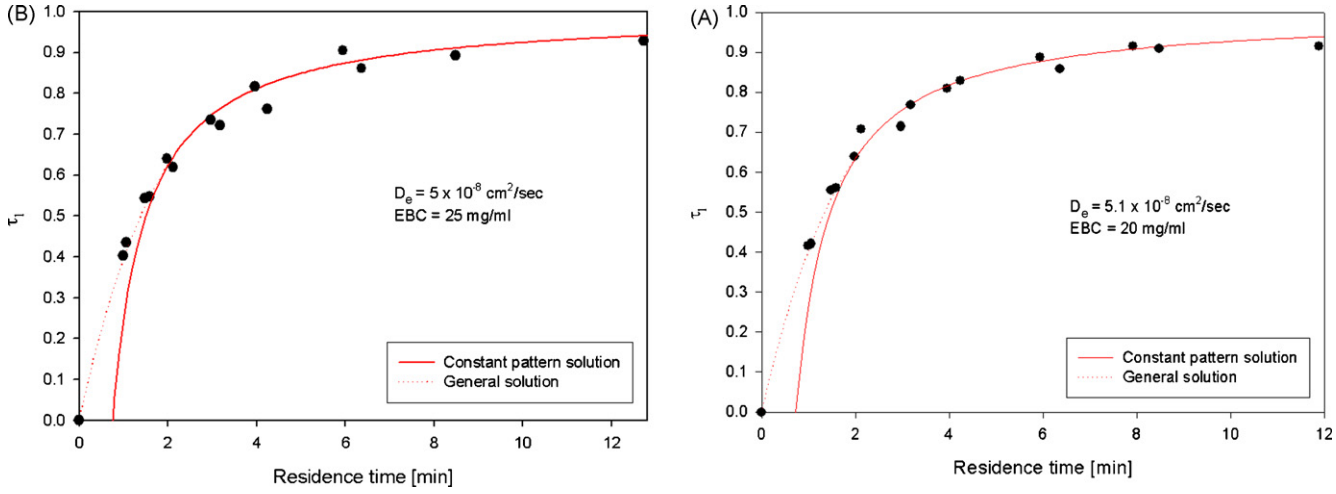

Fig. 6. Ratio of DBC to EBC (dimensionless time) at 0.4 mg/ml (A) and at 1 mg/ml polyclonal IgG (B). Calculation of effective diffusivity D_e by pore diffusion constant pattern model [12] and general solution model [13].

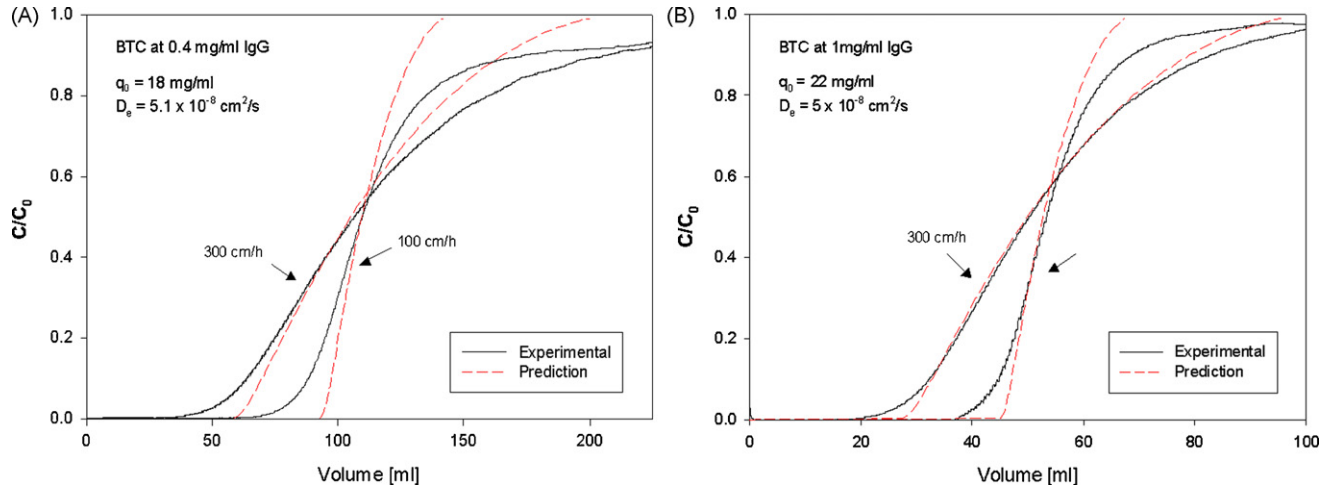

Fig. 7. Prediction of breakthrough with the film and pore diffusion model under constant pattern condition published by Weber and Chakravorti [20] at 0.4 mg/ml IgG (A) and 1 mg/ml IgG (B). Solid lines represent experimental data, dashed lines represent predicted data.

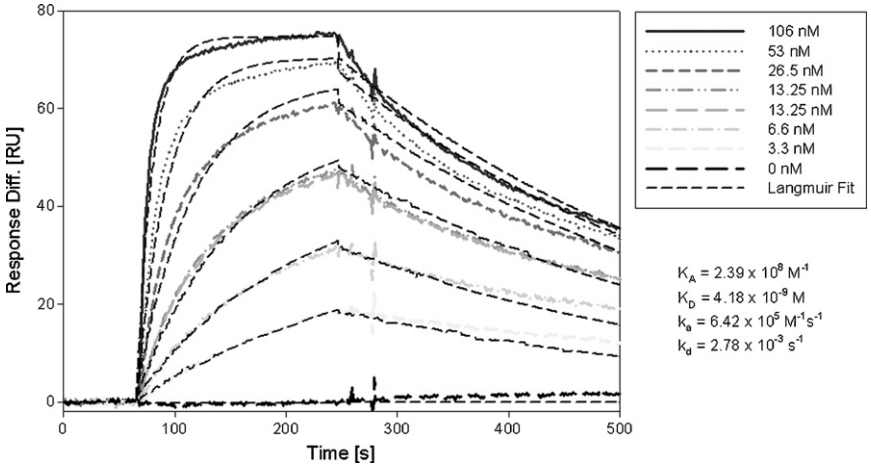

Fig. 8. Surface plasmon resonance kinetic measurements. 1000 RU IgG were immobilized on CM5 chip. Binding of CaptureSelect human-Fc-ligand in different concentrations was measured.

using a greater D_e value of 2×10^{-8} cm^2/s. Several groups could also describe the adsorption of IgG on SpA by a pore diffusion limited process [2,10].

4.4. Surface plasmon resonance

Kinetic parameters of the free CaptureSelect human IgG ligand were determined using the surface plasmon resonance (SPR) system Biacore 2000. IgG was immobilized onto a CM5 chip sensor surface by EDC/NHS chemistry with an amount of approximately 1000 RU. Various concentrations of CaptureSelect human-Fc-ligand were chosen in a manner that ensured an equilibrium binding signal $\leq$100 RU. The obtained sensorgrams were subtracted from the sensorgrams of a blank cell and evaluated with the Langmuir 1:1 binding model using Biocore software. Results are shown in Fig. 8. Table 2 provides a summary of kinetic parameters, measured from free camelid Fc-ligand in surface plasmon resonance and from immobilized camelid Fc-ligand on gel matrix by batch isotherm and batch uptake kinetic. Real biosensor data were also compared with those of the SpA domain Z published by Gülich et al. [27]. Saha et al. [28] measured adsorption kinetics of SpA by using an acoustic waveguide device (see also Table 2). As expected, higher kinetic rates than those from batch uptake kinetics were observed in SPR, due to the lack of pore diffusion on a chip surface. Detailed SPR affinity data of the camelid Fc-ligand for the several IgG subclasses were published from Klooster et al. [9]. The values are comparable with our data, obtained with polyclonal antibody. The K_A value of camelid Fc-ligand was determined one order of

Table 2
Summary of kinetic parameters, measured by using surface plasmon resonance from free ligand, and in batch adsorption experiments.

Binding system (method of measurement)	K_A (M^{-1})	K_D (M)	k_a (M^{-1} s^{-1})	k_d (s^{-1})
Free camelid Fc-ligand binding to immobilized IgG (surface plasmon resonance)	2.38×10^8	4.18×10^{-9}	6.42×10^5	2.78×10^{-3}
Immobilized camelid Fc-ligand on gel matrix (batch isotherm, batch uptake kinetics)	2.5×10^7	3.3×10^{-8}	5.4×10^2	2.2×10^{-5}
Free protein A domain Z binding to immobilized IgG[a] (surface plasmon resonance)	1.1×10^7	8.8×10^{-8}	7.8×10^4	6.9×10^{-3}
Free IgG binding to immobilized protein A[b] (acoustic waveguide device)	2.90×10^7	3.40×10^{-8}	8.02×10^3	2.77×10^{-4}

[a] Data from Gülich et al. [27].
[b] Data from Saha et al. [28].

magnitude greater than this of SpA, indicating a greater affinity. Adsorption rate constants from SpA and SpA domain Z are one or two orders of magnitude lower than these of the camelid Fc-ligand indicating a slower association.

The apparent or overall adsorption rate for non-linear isotherms can be described as a product of the adsorption kinetics, film diffusion and pore diffusion with the following equation [29,30]:

$$\frac{1}{k_a} \approx \frac{1}{k_a^{int}} + \frac{d_p q_{max}}{6k_f}\left(\frac{2+K_A c_0}{1+K_A c_0}\right) + \frac{d_p^2 q_{max}}{60 D_e} \quad (25)$$

total ≈ adsorption kinetics + film + pore.

where k_a represents the apparent adsorption rate (obtained from batch isotherm measurements), k_a^{int} the intrinsic adsorption rate constant (obtained from real time biosensor measurements), K_A the association constant (obtained from batch adsorption experiments) and c_0 the inlet concentration in the liquid. Parameters which are not explained are described in Section 3. The film mass transfer coefficient k_f was taken from literature as 0.0021 cm/s [2]. The reciprocal adsorption rate constant $1/k_a$ with approximately 2×10^{-3} M s is much greater than the reciprocal intrinsic adsorption rate $1/k_a^{int}$ constant with 1.5×10^{-6} M s. When estimating the contribution of pore diffusion, a value of 4.6×10^{-3} M s is obtained. This is in the same order of magnitude of $1/k_a$. The contribution of the overall adsorption rate limitation due to the film diffusion and adsorption on the surface is less than 3% and therefore negligible.

5. Conclusion remarks

We have completed the picture of camelid antibodies directed to the Fc-region of IgG by measuring the engineering parameters for optimal design of such an adsorption process. The camelid antibody column has slightly different engineering properties than conventional SpA affinity chromatography media; in particular a lower capacity of polyclonal IgG with 26 mg/ml compared to approximately 70 mg/ml of, *e.g.* MabSelectXtra SpA media was obtained. Camelid antibodies are monovalent molecules, whereas SpA has a theoretical valency of five, in fact a valency of 2–3 was determined in practice. Another explanation for lower capacity can be lower ligand density or lower surface area. Mass transfer could be described by using a film and pore diffusion model. With a value of $D_e = 5 \times 10^{-8}$ cm^2/s CaptureSelect human-Fc affinity matrix exhibited similar mass transfer behaviour as SpA media. Low et al. [24] evaluated the CaptureSelect human-Fc affinity matrix as the only alternative to SpA sorbents which offers similar selectivity. This is attributed to greater complexity in comparison to most commonly other IgG binding alternatives. Klooster et al. [9] have shown the successful application of this camelid antibody affinity matrix for immunoadsorption for treatment of immunological disorders. In some autoimmune diseases the IgG_3 fraction is increased. SpA lacks binding to IgG_3 and can therefore not be used for depletion. The application of CaptureSelect human-Fc affinity matrix maybe an alternative.

Nomenclature

c	protein concentration in mobile phase (mg/mL)
C	sample outlet concentration (mg/mL)
C_f	protein concentration in feed (mg/mL)
C_{ref}	reference concentration (mg/mL)
C_0	initial mobile phase protein concentration, feed concentration (mg/mL)
d_p	particle diameter (cm)
DBC	dynamic binding capacity (mg/mL)
DBC10%	dynamic binding capacity at 10% breakthrough (mg/mL)
D_e	effective diffusivity (cm^2/s)
D_0	free solution protein diffusivity (cm^2/s)
EBC	equilibrium binding capacity (mg/mL)
k_a	association rate constant (mL/mg s); (M^{-1} s^{-1})
k_d	dissociation rate constant (s^{-1})
k_f	film mass transfer coefficient (cm/s)
K	linear isotherm equilibrium constant (=q/c)
K_A	association constant (mL/mg); (M^{-1})
K_D	dissociation constant (mg/mL); (M)
L	column length (cm)
q	adsorbed protein concentration in the stationary phase (mg/mL)
$\bar{q}$	average concentration in particle (mg/mL)
q_{max}	maximum protein adsorption capacity (mg/mL)
q_s	saturated adsorbed-phase concentration (mg/mL)
r_p	particle radius (cm)
R	dimensionless separation factor
t	time (s)
u	superficial mobile phase velocity (cm/s)
v	volume of the stationary phase (mL)
V	volume of the mobile phase (mL)

Greek letters

ε	extraparticle void fraction
Λ	fraction of adsorbed protein at equilibrium; partition ratio
τ_1	dimensionless time

Dimensionless transport parameters

B_i	dimensionless Biot number (=$r_p k_f/D_e$)
N_{film}	number of transfer units for film mass transfer (=$6(1-\varepsilon)k_f L/u d_p$)
N_{pore}	number of transfer units for pore diffusion (= $60(1-\varepsilon)D_e L/u d_p^2$)
Sh	Sherwood number (=$k_f d_p/D_0$)

References

[1] C. Hamers-Casterman, T. Atarhouch, S. Muyldermans, G. Robinson, C. Hamers, E.B. Songa, N. Bendahman, R. Hamers, Nature 363 (1993) 446.
[2] R. Hahn, P. Bauerhansl, K. Shimahara, C. Wizniewski, A. Tscheliessnig, A. Jungbauer, J. Chromatogr. A 1093 (2005) 98.
[3] A.A. Shukla, B. Hubbard, T. Tressel, S. Guhan, D. Low, J. Chromatogr. B 848 (2007) 28.
[4] G. Fassina, M. Ruvo, G. Palombo, A. Verdoliva, M. Marino, J. Biochem. Biophys. Methods 49 (2001) 481.
[5] Z. Amoura, S. Koutouzov, H. Chabre, P. Cacoub, I. Amoura, L. Musset, J.F. Bach, J.C. Piette, Arthritis Rheum. 43 (2000) 76.
[6] E.I. Rigopoulou, E.T. Davies, D.P. Bogdanos, C. Liaskos, M. Mytilinaiou, G.K. Koukoulis, G.N. Dalekos, D. Vergani, Liver Int. 27 (2007) 1226.
[7] A. Staudt, M. Böhm, F. Knebel, Y. Grosse, C. Bischoff, A. Hummel, J.B. Dahm, A. Borges, N. Jochmann, K.D. Wernecke, G. Wallukat, G. Baumann, S.B. Felix, Circulation 106 (2002) 2448.
[8] M. Lauwereys, M.A. Ghahroudi, A. Desmyter, J. Kinne, W. Hölzer, E. De Genst, L. Wyns, S. Muyldermans, EMBO J. 17 (1998) 3512.
[9] R. Klooster, B.T.H. Maassen, J.C. Stam, P.W. Hermans, M.R. ten Haaft, F.J.M. Detmers, H.J. de Haard, J.A. Post, C. Theo Verrips, J. Immunol. Methods 324 (2007) 1.
[10] J.T. McCue, G. Kemp, D. Low, I. Quinones-Garcia, J. Chromatogr. A 989 (2003) 139.
[11] W.K. Teo, D.M. Ruthven, Ind. Eng. Chem. Proc. DD 25 (1986) 17.
[12] R.S. Cooper, D.A. Liberman, Ind. Eng. Chem. Fundam. 9 (1970) 620.
[13] G. Carta, A.R. Ubiera, T.M. Pabst, Chem. Eng. Technol. 28 (2005) 1252.
[14] H.C. Thomas, J. Am. Chem. Soc. 66 (1944) 1664.
[15] I. Langmuir, J. Am. Chem. Soc. 40 (1918) 1361.
[16] M.D. LeVan, G. Carta, C.M. Yon, in: R.H. Perry, D.W. Green (Eds.), Perry's Chemical Engineers' Handbook, McGrawHill, New York, 1997.
[17] G.L. Skidmore, B.J. Horstmann, H.A. Chase, J. Chromatogr. 498 (1990) 113.
[18] H.A. Chase, J. Chromatogr 297 (1984) 179.
[19] E.J. Wilson, C.J. Geankoplis, Ind. Eng. Chem. Fundam. 5 (1966) 9.
[20] T.W. Weber, R.K. Chakravorti, AIChE J. 20 (1974) 228.
[21] J.H. Petropoulos, A.I. Liapis, N.P. Kolliopoulos, J.K. Petrou, N.K. Kanellopoulos, Bioseparation 1 (1990) 69.

[22] A.K. Hunter, G. Carta, J. Chromatogr. A 937 (2001) 13.
[23] H. Yang, M.R. Etzel, Ind. Eng. Chem. Res. 42 (2003) 890.
[24] D. Low, R. O'Leary, N.S. Pujar, J. Chromatogr. B 848 (2007) 48.
[25] M.T. Tyn, T.W. Gusek, Biotechnol. Bioeng. 35 (1990) 327.
[26] B.J. Horstmann, H.A. Chase, Chem. Eng. Res. Des. 67 (1989) 243.
[27] S. Gülich, M. Uhlen, S. Hober, J. Biotechnol. 76 (2000) 233.
[28] K. Saha, F. Bender, E. Gizeli, Anal. Chem. 75 (2003) 835.
[29] A. Jungbauer, R. Hahn, J. Chromatogr. A 1184 (2008) 62.
[30] W.C. Li, J. Chromatogr. B 699 (1997) 29.